

Light storage and thermal-assisted switching of $\text{SrAl}_2\text{O}_4:\text{Eu}^{2+}, \text{Dy}^{3+}$

J. K. Adhinarta*, E. Jobiliong[†], M. Shiddiq[‡],
H. P. Uranus[§] and E. Steven^{*,¶,||}

**Applied Science Academy,
Sekolah Pelita Harapan,
Tangerang, Banten 15810, Indonesia*

*†Faculty of Science and Technology,
Universitas Pelita Harapan,
Tangerang, Banten 15810, Indonesia*

*‡Pusat Penelitian Fisika,
Lembaga Ilmu Pengetahuan Indonesia,
Tangerang Selatan, Banten 15314, Indonesia*

*§Department of Electrical Engineering,
Universitas Pelita Harapan,
Tangerang, Banten 15810, Indonesia*

*¶Laboratory for Interdisciplinary Science,
Emmerich Education Center,
Jakarta Utara, DKI Jakarta 14450, Indonesia
||eden.steven@gmail.com*

Accepted 24 January 2020

Published 10 March 2020

In this work, we demonstrate and evaluate the viability of $\text{SrAl}_2\text{O}_4:\text{Eu}^{2+}, \text{Dy}^{3+}$ crystals for long-term light storage applications at low temperatures that can be activated at higher temperatures for on-demand lighting applications. The switching mechanism is discussed from the point of view of the possible interplay between charge transport and the persistent luminescence in this system. Step-wise temperature-dependent luminescence decay time measurement is carried out to determine the optimal temperature for photo-charging and the operational temperature limit of the crystal-under-test as light sources.

Keywords: Phosphorescence; decay rate; temperature-dependent luminescence.

1. Introduction

$\text{SrAl}_2\text{O}_4:\text{Eu}^{2+}, \text{Dy}^{3+}$ crystals are among the materials that exhibit the most pronounced phosphorescence that is appealing for alternative lighting technologies that are independent, rechargeable, and energy efficient. Here, phosphorescence refers to

||Corresponding author.

the delayed emission of light around room temperatures (RTs) after excitation of the crystals by blue or UV light. The strontium aluminate phosphor possesses advantages over sulfide-based phosphors such as ZnS:Cu, as its afterglow can be observed by the (dark-adapted) eye for 18–24 h.¹ Ever since the first reported synthesis of the SrAl₂O₄:Eu²⁺, Dy³⁺,¹ countless variations^{2,3} of the doped double oxide SrO–Al₂O₃ and its derivatives have been synthesized and studied. Decades of research have shown the rich physics and the highly tunable nature of the structure-property relationships in this system.^{3–7} The crystal structure of SrAl₂O₄ is monoclinic. The unit cell comprises of four formula units where together they form eight AlO₄ tetrahedra that are linked through shared oxygen corners with four Sr²⁺ ions located among the tetrahedra.⁸ Dopant ions can be introduced to the host matrix SrAl₂O₄ where they occupy the Sr²⁺ sites. By altering the chemical composition, stoichiometry, and dopant ions of the system, it is possible to tune the color of luminescence,⁴ the temperatures at which the glow is optimal,^{5,6} the intensity and duration of afterglow,⁷ and more.⁹

These advances present an opportunity from alternative energy point of view. In this work, we consider the possibility of such crystals, in particular the SrAl₂O₄:Eu²⁺, Dy³⁺ as light-energy storage. Here, the key is to explore and evaluate the switching process to establish the rules for charging and discharging of the light, and to evaluate strategies that may help in improving the crystals as light-energy storage. For storage applications, it is necessary to prevent light emission after the photo-charging process. Secondly, it is necessary that even when the light emission is switched off after photo-charging process, the energy is retained and not wasted to non-radiative energy expenses. It is therefore important to understand and tie together the various models that have been proposed, to narrow down the key parameters that needs to be optimized in regard to using the strontium aluminate phosphor as light-storage.

In this work, we present a proof-of-concept of using the SrAl₂O₄:Eu²⁺, Dy³⁺ as light-energy storage. The light-storing is based on rapid thermal quenching to liquid nitrogen temperatures after photo-charging at RTs. To elucidate the mechanisms behind the suppression, various phosphorescence models are reviewed, where the key parameters relevant to light-storage capability is highlighted. A step-wise temperature-dependent luminescence measurement is carried out to investigate the persistent luminescence behavior at various temperatures. Finally, a brief recommendation is given for future research direction for improving the aluminate phosphors as light-energy storage.

2. Experimental Details

The SrAl₂O₄:Eu²⁺, Dy³⁺ is purchased commercially from CV. Indo Glow Dark. The source of irradiation or photoexcitation in all experiments is a commercial 400 nm laser diode with ~ 5 mW power. The luminescence spectra was recorded using Maya2000 Pro Spectrometer (symmetric crossed Czerny–Turner spectrometer

with 200–1100 nm spectral range). The spectra are collected every second using a custom-programmed LabView interface.

For the temperature-dependent luminescence decay time measurements, the setup must be able to stabilize the temperature of the sample while maintaining the photo-charging/discharging cycles over a fixed time period. In this experiment, we utilized a NiChrome heating coil to regulate the temperature using programmatic PID modules (see Fig. A.1). A thermocouple is connected to Picotest M3510A with GPIB interface and connected to a computer to acquire the temperature readings. Light-intensity was measured via the voltage of a light-dependent-resistor voltage divider circuit. The experiment was done under vacuum in order to isolate the temperature variation to only the sample and thermocouple.

The PID controller was set to regulate temperatures between 27°C and 120°C at 1°C increments in each photo-charging/-discharging cycle. In this experiment, the excitation period was set to be 5 s long. A new charging cycle started once the light-intensity measurement dropped below a certain threshold. The setup was automated via LabView, in order to simultaneously regulate the temperature, control the photo-excitation cycles, and to measure the light intensity of the sample throughout the experiment.

Luminescence intensity and luminescence decay time constants were extracted programmatically from the cyclic temperature-dependent data using an IgorPro custom-script.^a Here, auto-peak identification algorithm is employed to recognize the beginning of each photo-charging/discharging cycles. From there, exponential fit is done to extract the time constants of the decay.

3. Results and Discussions

Here, we demonstrate the utilization of SrAl₂O₄:Eu²⁺, Dy³⁺ crystals as light-energy storage by carrying out the following simple procedure. First, crystals are photo-charged using blue light (400 nm) at RTs. Then, the crystals are rapidly quenched to liquid nitrogen bath to ~80 K temperatures. As shown in Fig. 1(a), this results in an instant suppression of the light emission. What is remarkable is that even after more than 6 h (in this test) being kept at low temperatures and in the dark, that the crystals re-glow when they are brought back to RTs.

We also confirm that there are two distinct emissions by the crystals. The first type is referred to as photoluminescence which is shown in Fig. 1(a) as the bright and intense green spot of the crystal being subjected to the laser source. In Fig. 1(b), the spectra after the excitation of the crystals under blue light is shown. Two peaks are observed. First peak around 400 nm is due to the reflection of the laser source. The second peak around 520 nm is due to the photoluminescence of the crystals. This peak disappears almost instantaneously to a much lower intensity value (Fig. 1(b)), after which, an afterglow (hereafter referred to as persistent luminescence) is

^aCode is available at www.github.com/jasonkena/ThermalSwitching.

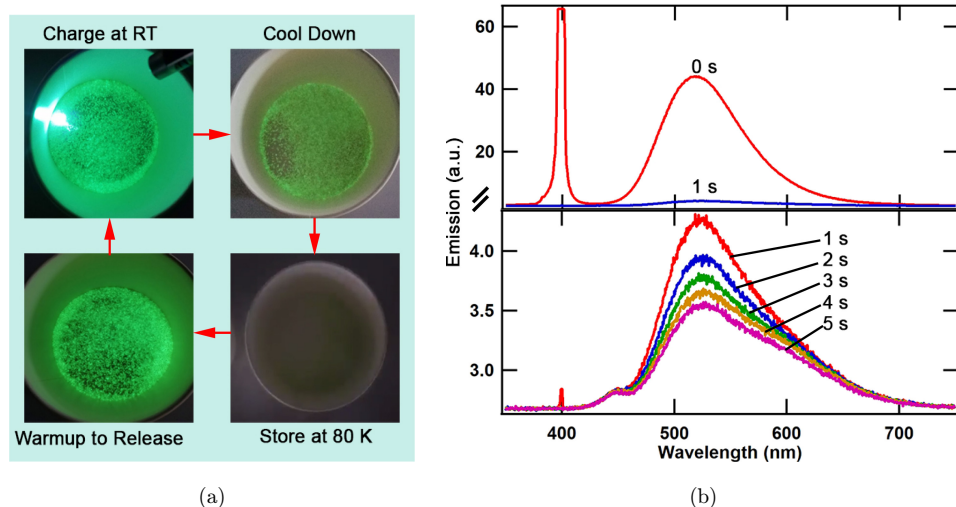


Fig. 1. (Color online) Light-storing demonstration and luminescence spectra of the $\text{SrAl}_2\text{O}_4:\text{Eu}^{2+}, \text{Dy}^{3+}$. (a) Photo-charging/-discharging scheme: (top-left) charging at RT; (top-right and bottom-right) storing at low temperature; (bottom-left) photo-discharging at RT. This cyclic process can be reinitiated as necessary. (b) Top: photoluminescence spectra. Red and blue curves denote the spectra of the crystal while under blue light (~ 400 nm) excitation (at 0 s) and 1 s after the excitation source is turned off, respectively, showing an intense absorption at ~ 520 nm followed by a major intensity decrease. Bottom: persistent luminescent spectra at $t = 1-5$ s. A more gradual and much slower decrease in the ~ 520 nm absorption intensity is shown. A small peak ~ 450 nm may indicate a small amount of $\text{CaAl}_2\text{O}_4:\text{Eu}^{2+}$ impurity¹⁰ in the system.

observed. The persistent luminescence which also coincides at ~ 520 nm is decaying at a much slower rate as shown in Fig. 1(b). The 520 nm absorption peak is commonly observed in Eu^{2+} doped and also Dy^{3+} co-doped SrAl_2O_4 systems. It is assigned to the excitation and relaxation of Eu^{2+} ion as the luminescence centre.^{1,5}

Besides the suppression of the persistent luminescence at ~ 80 K, we also observe an enhanced photoluminescence at such temperatures (Fig. 2). Indeed, there is an interplay between the photoluminescence and persistent luminescence. At ~ 80 K, the photoluminescence is strong but the persistent luminescence is strongly

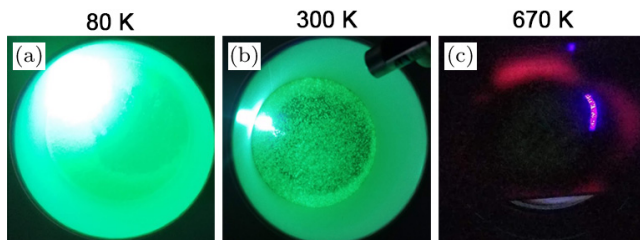


Fig. 2. (Color online) Photoluminescence evolution from low to high temperatures. Photographs of blue light irradiation at (a) 80 K, (b) 300 K, and (c) 670 K, showing strong, moderate, and complete suppression of photoluminescence, respectively.

suppressed. On the contrary, at RTs (~ 300 K), the photoluminescence is only moderate but the persistent luminescence is very strong. At higher temperatures (~ 670 K) both the photoluminescence and persistent luminescence completely vanish.

3.1. Interplay between photoluminescence and persistent luminescence

The suppression of the persistent luminescence at low temperatures has previously been observed by Chernov *et al.*¹¹ Similar to our case, when blue light (~ 400 nm) is used as irradiation source, a clear suppression of persistent luminescence is observed at ~ 20 K. As the temperature is raised above ~ 100 K, persistent luminescence begins to strengthen accompanied by a decreasing intensity of the photoluminescence. The decreasing photoluminescence intensity is discussed as due to unknown non-radiative loss for the excited electron in the Eu^{2+} ions as temperature is increased. As for the persistent luminescence, it is associated with recombination of trapped electron and hole.¹¹ Although the mechanisms for both photoluminescence and persistent luminescence are discussed, due to the various models being proposed and later debunked, the governing physics behind the interplay between the photoluminescence and persistent luminescence remains unrevealed.

3.2. Charge transport as key parameter for controlling charge trapping/de-trapping rate

Indeed, it is a very complicated situation. The nature of the traps mentioned above that act as a storage for supplying the persistent luminescence and the type of species being trapped (either electron or hole) are still being debated.^{1,2,9,12-15} The complications in figuring out the mechanisms are due to the complex system that consists of the host matrix (namely the aluminate oxides), the dopants (in this case the Eu^{2+}), and co-dopants (the Dy^{3+}). The undoped host matrix SrAl_2O_4 is not luminescent, until it is doped with rare-earth ions such as Eu^{2+} .¹² In $\text{SrAl}_2\text{O}_4:\text{Eu}^{2+}$, there are two distinct luminescent phenomena. When one excites the crystal with blue or UV light at RTs, a bright photoluminescent emission around 520 nm is observed. Right after the light source is turned off, the glow intensity decreases rapidly to a level after which, the persistent luminescence is observed. Finally, when the $\text{SrAl}_2\text{O}_4:\text{Eu}^{2+}$ is further co-doped with Dy^{3+} ions, an order of magnitude increased is observed in the persistent luminescence intensity and lifetime.¹

Although the origin of the 520 nm absorption peak in both doped and co-doped system is widely accepted as due to the intrinsic $5f - 4d$ transition of the Eu^{2+} in the system, the origin for the persistent luminescence remains elusive.^{1,9,12-15} Several decades of work have revealed more and more details that revises previous models. First, Matsuzawa model¹ relies on the evidence of the dominance of hole transport¹² in the system in the earlier work. It was proposed that when light excites the system, electron hole pairs are generated where the electron turns the Eu^{2+} into Eu^+ species, and the same time, a hole jumps into the valence band where it subsequently

migrates and jumps back out from the valence band into the Dy^{3+} turning it into Dy^{4+} species. At RTs, the trapped hole is then thermally-bleached and the reverse process then occurs where the electron-hole pair recombines which relaxes the Eu^{2+} ion resulting in luminescence.

The hole-based trapping mechanism was argued by Dorenbos¹³ who pointed out that hole transport is only possible in the case where electron is fully ionized from valence to conduction band which was not the case. He instead proposed an electron-based migration from the Eu^{2+} sites through conduction band into the Dy^{3+} trapping sites. Here, the stable luminescent and trapping centers are Eu^+ and Dy^{4+} , respectively, which are more energetically favorable.¹³

In both Matsuzawa and Dorenbos models, the links between the main luminescence centers and the trapping centers are either through the valence or conduction band depending on whether the charge carriers responsible are holes or electrons respectively. This direct link between the two centers is supported by strong correlation between photoconductivity and persistent luminescence behavior¹² in the $\text{SrAl}_2\text{O}_4:\text{Eu}^{2+}$, Dy^{3+} , suggesting that charge transport is one of the key factors that controls the rate of trapping or de-trapping regardless of whether the charge carrier is electron or hole. More work, however is required to investigate this interplay. Other models, for example those proposed by Aitasalo *et al.*¹⁰ and Clabau *et al.*⁵ do not rely on the charge transport as the main driver for trapping.

From light-energy storage point of view, if proven to be true, the link between the charge transport and the rate of trapping is very intriguing. This suggests that the key switch to accessing the storage for photo-charge/-discharge (here, we refer to the trapping centers being accessible or closed) may rely on the ability to control the charge transport behavior of the system. One very exciting idea is to tune the transport behavior of the crystals via electrical gating, like those in field-effect-transistors. In this approach, we take advantage of the fact that at lower temperatures, the charge transport in the aluminates host matrix is highly insulating due to its being a semiconductor, therefore suppressing the movement of trapped charges. More rigorous work proving the linkage between the charge transport and the persistent luminescence is however needed.

3.3. Operational parameter consideration

From an operational perspective, two factors are considered in using the crystal as lighting or light-energy storage. First is at what temperature will the crystal glow the most efficiently or brightest. Second, at what temperature will the photo-charging give the deepest charging in a given time. As a general rule, at higher temperatures, more intense glow is observed but the glow is short-lived due to availability of thermal energy to de-trap the charges. On the other hand, at lower temperatures, less intense glow is observed but the glow is longer-lasting due to the lack of thermal energy. In the aluminate phosphors however there exist a peak intensity at a given temperature where the persistent luminescence produced the strongest glow. This

temperature is known as the thermoluminescence peak. For example, in $\text{SrAl}_2\text{O}_4:\text{Eu}^{2+}, \text{Dy}^{3+}$ crystals grown by Clabau *et al.* in their work,⁵ the thermoluminescence peak temperature, T_{max} , is at $\sim 40^\circ\text{C}$. This suggests that around 40°C the trapped charges are most efficiently de-trapped for recombination at the Eu^{2+} luminescence centers. T_{max} can also be seen as the maximum temperature for operating the crystal as light source. Above T_{max} it is likely that some energy will be lost to non-radiative energy dissipation^{12,15} therefore decreasing the efficiency for light-emission. For practical purposes, therefore the crystal as light source is suitable for operation below T_{max} , 40°C in this case. From T_{max} and decay time constant, the activation energy of the trapping centers, E_T , can also be estimated by calculating E_T from Eq. (3.1),⁵

$$\frac{1}{\tau} = s \cdot e^{-\frac{E_T}{k_B T}}, \quad (3.1)$$

where s is a proportional factor to the vibration frequency of the trapped charges ($\sim 10^{12}\text{s}^{-1}$),⁵ τ is the persistent luminescence decay time constant, E_T is activation energy of the trap, k_B is Boltzmann constant, and T is temperature. In their case,⁵ the trap activation energy is estimated to be $\sim 0.62\text{ eV}$.

3.4. Step-wise temperature-dependent persistent luminescence measurement

In our experiment, a step-wise temperature-dependent luminescence measurement is employed. Briefly, the crystals undergo irradiation and relaxation process at every set constant temperature. In Fig. 3(a), we show the time-dependence of the light-intensity decay cycles. Each irradiation/relaxation cycle is taken at a set constant temperature. After each irradiation/relaxation cycles, the temperature is increased by 1°C where the next irradiation/relaxation cycle begin again; data is collected from 27°C to 120°C (Fig. 3(a)). Three parameters are extracted from this set of data. First is the thermoluminescence peak temperature, T_{max} . Second, the photo-charging temperature that results in the largest light exposure of the persistent luminescence, T_{charge} . Here, the light exposure is obtained by integrating decay curves during the persistent luminescence duration. Finally, the temperature dependence to the persistent luminescence decay time constant, τ .

In Fig. 3(b), the intensity after the initial 2 s of decay is plotted against temperature. The 2 s offset (also applies to analysis in Figs. 3(c) and 3(d)) is to account for the initial photo-emission due to photoluminescence (Fig. 1(b)) in order to narrow the evaluation to just the persistent luminescence. The T_{max} of our $\text{SrAl}_2\text{O}_4:\text{Eu}^{2+}, \text{Dy}^{3+}$, is $\sim 83^\circ\text{C}$. By using equation Eq. (3.1) with $\tau \sim 4.5\text{ s}$ (Fig. 3(d)), E_T is estimated to be $\sim 0.89\text{ eV}$. These values are higher than the crystals grown by Clabau *et al.*⁵ This may result from different processing conditions used by the sample grower, for example, it has been shown that ionization potential of the co-dopants⁵ or crystal synthesis temperature conditions¹⁵ affect the thermoluminescence behavior of the crystal. The crystal is therefore best operated below or at 83°C for lighting purposes.

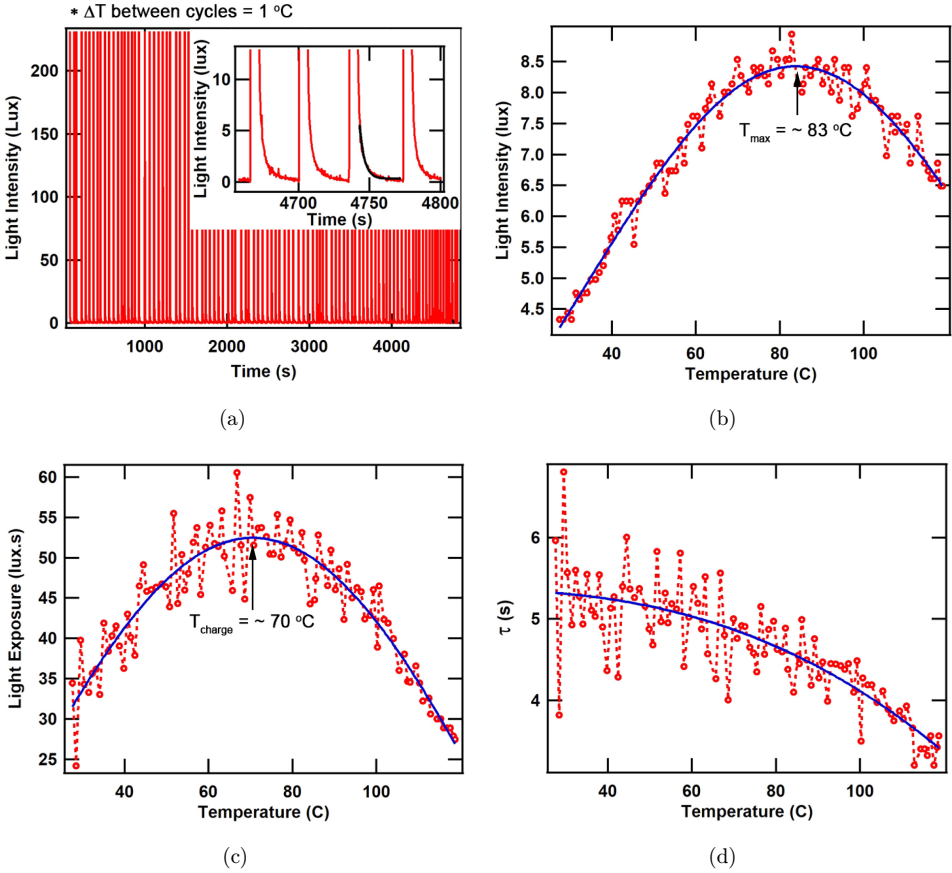


Fig. 3. (Color online) Temperature-dependent step-wise persistent luminescent measurement. (a) Photo-charging/-discharging cycles at step-wise constant temperatures, increment every 1°C from 27°C to 120°C . During each cycle, the sample temperature is kept constant. Inset: zoom-view of the cycle curves showing the exponential decay of the persistent luminescence. Black line: exponential fit for extracting τ . (b) Extracted intensity of the persistent luminescence against temperature. (c) Integrated decay curve vs temperature. (d) Temperature dependence of τ . In parts (b), (c), and (d), parameters are extracted based on light emissions 2 s after turning off the photoexcitation. Blue lines: guides are added for clarity.

In Fig. 3(c), the light exposure is plotted against temperature where a maxima is observed. Here, crystals that produce largest light exposure are thought to have undergone the deepest photo-charging. The optimal temperature for photo-charging that results in the deepest charge, T_{charge} , is therefore determined to be $\sim 70^\circ\text{C}$ (Fig. 3(c)).

Finally, we extract the time decay constants of the curves and plot it against temperature as shown in Fig. 3(d). We observe a decreasing trend as temperature is increasing which means that the energy discharges faster at higher temperature. This is expected due to thermal-bleaching of the trapping centers.¹ Based on these data, for our sample-under-test, the optimal operating conditions are to photo-charge the crystals at $\sim 70^\circ\text{C}$, store at $\sim -193^\circ\text{C}$ ($\sim 80\text{K}$), and use at temperatures below $\sim 83^\circ\text{C}$.

4. Conclusion

We have demonstrated and evaluated the viability of $\text{SrAl}_2\text{O}_4:\text{Eu}^{2+}, \text{Dy}^{3+}$ as light-energy storage. The rules for using the crystal as light-energy storage is simple: (1) charging is best done at T_{charge} ; (2) keep the crystal at low temperatures, $\sim 80 \text{ K}$, to suppress the trap activities; (3) use the crystals at or below T_{max} . In our case, the absorbed light-energy can be stored at least for up to 6 h. Based on the review of various models, it remains a possibility that the suppression of trap activities at trapping centers are directly influenced by the charge transport behavior of the host matrix. If direct linkage between the charge transport and trap activities is proven to be true, this could open up a new opportunity to improve the switching mechanism to become that of a field-effect-transistor. So instead of lowering/increasing the temperature, switching can be done at RTs via electric field gating. Admittedly, more work is required to verify this possibility.

Acknowledgments

We acknowledge the generous support of the Yayasan Pelita Harapan and Emmerich Education Center for the access to the research facilities. We thank the organizers of and speakers at ISMOA 2019 for discussions and suggestions during our investigation.

Appendix A. Experimental Setup

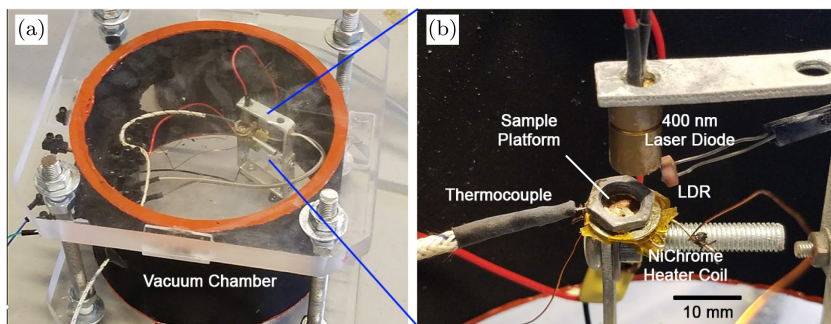


Fig. A.1. Experimental setup for temperature-dependent luminescence measurements. (a) Photographs of the vacuum chamber that houses the sample configurations and (b) the sample platform attached to a thermocouple, copper base, and NiChrome heater coil. Laser diode with 400 nm irradiation is used as excitation source. Light dependent resistors (LDR) are connected in voltage divider configurations with a reference 2 k Ω resistor. The LDR voltage variations at various temperatures are monitored and converted into resistance and then to lux by using a calibration equation of $I = 10^4 (R_{\text{LDR}} \cdot 10^4)^{-4/3}$, where I is light intensity, and R_{LDR} is the resistance of the LDR.

References

1. T. Matsuzawa, Y. Aoki, N. Takeuchi and Y. Murayama, A new long phosphorescent phosphor with high brightness, $\text{SrAl}_2\text{O}_4:\text{Eu}^{2+}, \text{Dy}^{3+}$, *J. Electrochem. Soc.* **143**(8) (1996) 2670–2673.

2. S. Poort, W. Blokpoel and G. Blasse, Luminescence of Eu^{2+} in barium and strontium aluminate and gallate, *Chem. Mater.* **7**(8) (1995) 1547–1551.
3. H. Luitel, T. Watari, R. Chand, T. Torikai and M. Yada, Giant improvement on the afterglow of $\text{Sr}_4\text{Al}_{14}\text{O}_{25}:\text{Eu}^{2+}$, Dy^{3+} phosphor by systematic investigation on various parameters, *J. Mater.* **2013** (2013) 1–10.
4. T. Katsumata, K. Sasajima, T. Nabae, S. Komuro and T. Morikawa, Characteristics of strontium aluminate crystals used for long-duration phosphors, *J. Am. Ceramic Soc.* **81**(2) (1998) 413–416.
5. F. Clabau, X. Rocquefelte, S. Jobic, P. Deniard, M.-H. Whangbo, A. Garcia and T. Le Mercier, On the phosphorescence mechanism in $\text{SrAl}_2\text{O}_4:\text{Eu}^{2+}$ and its codoped derivatives, *Solid State Sci.* **9**(7) (2007) 608–612.
6. B. M. Mothudi, O. Ntwaeaborwa, A. Kumar, K. Sohn and H. Swart, Phosphorescent and thermoluminescent properties of $\text{SrAl}_2\text{O}_4:\text{Eu}^{2+}$, Dy^{3+} phosphors prepared by solid state reaction method, *Phys. B: Condens. Matter* **407**(10) (2012) 1679–1682.
7. S.-D. Han, K. C. Singh, T.-Y. Cho, H.-S. Lee, D. Jakhari, J. P. Hulme, C.-H. Han, J.-D. Kim, I.-S. Chun and J. Gwak, Preparation and characterization of long persistence strontium aluminate phosphor, *J. Lumin.* **128**(3) (2008) 301–305.
8. M. Nazarov, M. Brik, D. Spassky, B. Tsukerblat, A. N. Nazida and M. Ahmad-Fauzi, Structural and electronic properties of $\text{SrAl}_2\text{O}_4:\text{Eu}^{2+}$ from density functional theory calculations, *J. Alloys Compd.* **573** (2013) 6–10.
9. M. Akiyama, C.-N. Xu, Y. Liu, K. Nonaka and T. Watanabe, Influence of Eu, Dy co-doped strontium aluminate composition on mechanoluminescence intensity, *J. Lumin.* **97**(1) (2002) 13–18.
10. T. Aitasalo, P. Dereń, J. Hölsä, H. Jungner, J.-C. Krupa, M. Lastusaari, J. Legendziewicz, J. Niittykoski and W. Stręk, Persistent luminescence phenomena in materials doped with rare earth ions, *J. Solid State Chem.* **171**(1–2) (2003) 114–122.
11. V. Chernov, T. Pipers, R. Meléndrez, W. Yen, E. Cruz-Zaragoza and M. Barboza-Flores, Photoluminescence, afterglow and thermoluminescence in $\text{SrAl}_2\text{O}_4:\text{Eu}^{2+}$, Dy^{3+} irradiated with blue and uv light, *Radiat. Meas.* **42**(4–5) (2007) 668–671.
12. V. Abbruscato, Optical and electrical properties of $\text{SrAl}_2\text{O}_4:\text{Eu}^{2+}$, *J. Electrochem. Soc.* **118**(6) (1971) 930–933.
13. P. Dorenbos, Mechanism of persistent luminescence in Eu^{2+} and Dy^{3+} codoped aluminate and silicate compounds, *J. Electrochem. Soc.* **152**(7) (2005) H107–H110.
14. H. Terraschke, M. Suta, M. Adlung, S. Mammadova, N. Musayeva, R. Jabbarov, M. Nazarov and C. Wickleder, $\text{SrAl}_2\text{O}_4:\text{Eu}^{2+}$, (Dy^{3+}) nanosized particles: Synthesis and interpretation of temperature-dependent optical properties, *J. Spectrosc.* **2015** (2015) 541958–541958.
15. D. Haranath, V. Shanker, H. Chander and P. Sharma, Studies on the decay characteristics of strontium aluminate phosphor on thermal treatment, *Mater. Chem. Phys.* **78**(1) (2003) 6–10.